TRIUMF

Methods of Designing a Synchrotron Lattice with High Transition Energy

Ramesh C. Gupta

This work has been done under the supervision of Drs. M.K. Craddock and J.I.M. Botman in the Accelerator Research Division at TRIUMF during the period of May 1983 to December 1983 for the M.Sc. Course in Accelerator Physics at the University of Manitoba.

TRIUMF
4004 Wesbrook Mall
Vancouver, B.C. V6T 2A3

February 1984

Acknowledgements

I wish to express my sincere appreciation to Drs. M.K. Craddock and J.I.M. Botman for their continual guidance and encouragement during the course of this work and in preparing this report.

I wish to thank Dr. R. Servranckx of the University of Saskatchewan for much helpful advice, especially in connection with using the lattice code DIMAT. The assistance of the members of the computing services, and Fred Jones in particular, has been very valuable.

TRIUMF	4004 WESBROOK MALL, UBC CAMPUS, VANCOUVER, B.C. V6T 2A3			
DESIGN NOTE	NAME Ramesh C. Gupta	DATE December 1983	FILE NO. TRI-DN-83-51	PAGE 1

SUBJECT Methods of Designing a Synchrotron Lattice with High Energy Transition Energy

Abstract

In this report various methods of designing a synchrotron lattice with high transition energy are described. All schemes are based on making a periodic lattice with the number of periods n just above the horizontal tune of the machine. An nth harmonic component is introduced by modulating either the focusing or the bending fields or both in each period. Ways to generate this modulation are explored and the effects on the lattice functions examined. Some of the methods provide long drift spaces or straight sections which may be utilized for injection, extraction, RF acceleration etc.

BP81411

TRIUMF	4004 WESBROOK MALL, UBC CAMPUS, VANCOUVER, B.C. V6T 2A3			
DESIGN NOTE	NAME Ramesh C. Gupta	DATE December 1983	FILE NO. TRI-DN-83-51	PAGE 2

SUBJECT Methods of Designing a Synchrotron Lattice with High Energy Transition Energy

Contents

BP81-411

1. Introduction

In most proton synchrotrons the energy of the particles crosses a value, known as transition energy E_t, at which there is no phase stability. In high current synchrotrons the beam loss near the transition energy due to space charge defocusing forces and beam instabilities becomes important. A way to circumvent this problem is to design a synchrotron lattice in such a way that E_t stays out of the energy range of the machine. In this report we describe methods of designing such a lattice.

For the TRIUMF Kaon factory a 30 GeV, 100 μA synchrotron[1)] consisting of CERN/ISR magnets has been proposed. A regular lattice with E_t in the range of acceleration is given in fig. 1. It was suggested by H.G. Hereward[2)] to design the lattice for this machine with high E_t, employing a set of trim quadrupoles. In this report several possible lattices using different methods for achieving high E_t are described. The present lattice for this proposal is explained in more detail. It provides many long drift spaces by rearranging the dipole spacing and thus eliminates the need for additional ~~quadrupoles or~~ straight sections[3)]. The lattice code DIMAT[15)] of R. Servranckx has been extensively used for this work; this code computes the lattice functions and particle trajectories in a circular machine using a second order matrix formalism.

2. Theory

In section 2.1 we investigate problems at the transition energy in a high current synchrotron and explain the need for designing a high transition energy lattice for the TRIUMF Kaon Factory Synchrotron. In section 2.2 we briefly review the theory of strong focusing synchrotrons given by Courant and Snyder[4)], especially regarding the derivation of the expressions for the transition energy. In section 2.3 we discuss the basic principle of changing the transition energy and in section 2.4 we examine the effects on the lattice functions.

2.1 Phase Stability and Transition Energy

In synchrotrons the acceleration of particles having a nonsynchronous energy or a nonsynchronous phase is possible due to the mechanism of phase stability[5,6)], provided that the deviations in energy and phase are not too large. Consider the difference Δτ in the revolution period τ due to a difference ΔC in orbit circumference C and Δv in velocity v between a nonsynchronous particle with momentum p+Δp and synchronous particle with momentum p:

$$\frac{\Delta\tau}{\tau} = \frac{\Delta C}{C} - \frac{\Delta v}{v} \quad .$$

The momentum compaction factor α is defined as the relative change in circumference due to a relative change in momentum:

$$\alpha = \frac{\Delta C/C}{\Delta p/p} \quad .$$

Using this and

$$\frac{\Delta v}{v} = \frac{1}{\gamma^2} \frac{\Delta p}{p} ,$$

where $\gamma = E/E_0$ with E_0 the rest energy, one obtains

$$\frac{\Delta \tau}{\tau} = (\alpha - \frac{1}{\gamma^2}) \frac{\Delta p}{p} \equiv \eta \frac{\Delta p}{p} ,$$

thus defining the quantity η.

In most strong focusing proton synchrotrons (see Eq. (13) below) α has a value such that η increases from negative to positive during acceleration. The energy at which η becomes 0 is called the transition energy $E_t = E_0\gamma_t$ and $\gamma_t = 1/\sqrt{\alpha}$.

The quantity η, which gives the connection between momentum and phase errors, is directly proportional to the strength of phase focusing. Below transition energy $\eta < 0$ and phase stability (focusing) exists if the synchronous phase is chosen on the rising side of the RF voltage curve. Above transition η is positive and phase stability can be restored again if the synchronous phase is shifted towards the falling side of the RF voltage curve. At transition energy $\eta = 0$, meaning no phase focusing to keep the bunch compressed. However $|\eta|$ also determines the bunch length which is shortest when $\eta = 0$.

In low current synchrotrons the change in RF phase causes almost no beam loss since the bunch is shortest at transition and the time required for the phase change is very small w.r.t. the time scale of phase oscillations. However, in a high current synchrotron the situation becomes different due to

(a) space charge defocusing forces (maximum at transition when the bunch is shortest), disturbing the bunch length,

(b) space charge forces enhancing beam instabilities at transition;

Thus beam loss may become important.

These problems become significant at beam intensities about 1% of those under consideration for a TRIUMF Kaon factory. At the CERN PS a sophisticated γ_t-jump scheme has been implemented[7)] to allow 3×10^{13} ppp to be accelerated through transition. For TRIUMF's aim of 6×10^{14} ppp, however, it seemed desirable to design a lattice with γ_t outside the acceleration range, if possible.

2.2 Review of the theory of strong focusing synchrotrons

The equation of horizontal motion for charged particles with momentum $p + \Delta p$ in a static magnetic field is given by

$$\frac{d^2x}{ds^2} + \left[\frac{1}{\rho^2(s)} - K(S)\right] x = \frac{1}{\rho(s)} \frac{\Delta p}{p} . \tag{1}$$

The path variable s runs from 0 to C (the circumference of the machine) and x is the deviation from the equilibrium orbit. The dispersion function η_x represents the deviation for the particle with $\Delta p/p = 1$

or $$\eta_x = \frac{x}{\Delta p/p} . \tag{2}$$

Furthermore ρ is the bending radius and K the focusing strength on the equilibrium orbit and these variables satisfy the periodicity conditions:

$$\rho(s + C) = \rho(s),$$
$$K(s + C) = K(s).$$

In addition if the machine is constructed of n identical sections then

$$\rho(s + C/n) = \rho(s),$$
$$K(s + C/n) = K(s), \tag{3}$$

is also satisfied. These sections may either be individual magnet cells, or a super-period consisting of several cells. The solution of eq. (1) for $\Delta p = 0$ then may be expressed in the form of the so called Twiss matrix M

$$\begin{pmatrix} x(s) \\ x'(s) \end{pmatrix} = M \begin{pmatrix} x(0) \\ x'(0) \end{pmatrix},$$

where $x' \equiv dx/ds$ and

$$M(s) = \begin{pmatrix} \cos\mu + \alpha \sin\mu & \beta \sin\mu \\ -\gamma \sin\mu & \cos\mu - \alpha \sin\mu \end{pmatrix}, \tag{4}$$

where $\beta(s)$ is the envelope function, $\alpha = -\beta'/2$, $\gamma = (1+\gamma^2)/\beta$ and $\mu(s) = \int_0^s ds/\beta$ is the phase advance. The particles with momentum p can have a maximum displacement $\sqrt{\beta\varepsilon}$ where $\pi\varepsilon$ is the horizontal emittance.

To solve the inhomogenous equation ($\Delta p \neq 0$) we first apply the Floquet transformation:

$$\xi = \beta^{-1/2} x,$$
$$d\phi = \frac{ds}{\nu\beta} , \tag{5}$$

where ϕ is the normalized phase advance (2π in one complete orbit), ν is the betatron tune and $\mu = \nu\phi$ and Eq. (1) transforms to

$$\frac{d^2\xi}{d\phi^2} + \nu^2\xi = \nu^2 \frac{\beta^{3/2}}{\rho} \frac{\Delta p}{p} . \tag{6}$$

This equation can be solved by expanding $\beta^{3/2}/\rho$ in a fourier series:

$$\frac{\beta^{3/2}}{\rho} = \sum_{k=-\infty}^{\infty} a_k e^{-ik\phi} , \tag{7}$$

with $$a_k = \frac{1}{2\pi}\int_{-\pi}^{\pi} \frac{\beta^{3/2}}{\rho} e^{-ik\phi} d\phi ; \tag{8}$$

one obtains $$\xi = \frac{\Delta p}{p} \nu^2 \sum_k \frac{a_n e^{ik\phi}}{\nu^2 - k^2} . \tag{9}$$

Therefore the change in circumference ΔC for the off momentum particle is

$$\Delta C = \int_0^C \frac{x}{\rho} ds = \nu\int_{-\pi}^{\pi} \frac{\beta^{3/2}}{\rho} \xi d\phi = 2\pi\nu^3 \frac{\Delta p}{p} \sum_k \frac{|a_k^2|}{\nu^2 - k^2} . \tag{10}$$

Using the definition of compaction factor (section 2.1) one obtains

$$\alpha = \frac{\nu^3}{R}\sum_k \frac{|a_k{}^2|}{\nu^2-k^2} , \tag{11}$$

where R is the average radius of the machine with $C = 2\pi R$.

In most synchrotron designs the leading term is the one with $k = 0$. Using the approximation that β can be replaced by its average value (R/ν) in eq. (8)

$$a_o = \frac{1}{2\pi}\int \frac{\beta^{3/2}}{\rho} d\phi = \frac{1}{2\pi\nu}\int_0^C \frac{\beta^{1/2}}{\rho} ds \simeq \left(\frac{R}{\nu^3}\right)^{1/2} . \tag{12}$$

Therefore in most synchrotron designs

$$\alpha \simeq \frac{1}{\nu^2}. \tag{13}$$

Since $\gamma_t = 1/\sqrt{\alpha}$, the harmonic $k = 0$ gives

$$\gamma_t \simeq \nu . \tag{14}$$

If instead there is an additional major contribution from the harmonic $k = n$ (and therefore also from $k = -n$) then

$$\frac{1}{\gamma_t^2} \simeq \frac{1}{\nu^2}\left[1 + 2\ |a_n^2|\ \frac{\nu^3}{R}\ \frac{\nu^2}{\nu^2-n^2}\right], \tag{15}$$

neglecting the contributions from other harmonic components. The factor 2 takes care of the contributions from $|a_n|$ and $|a_{-n}|$.

To compute a_n due to errors $k(s)$ in the field gradients we quote the following results of Courant and Snyder.

Defining $J_n = \int_o^c \beta(s)\ k(s)\ e^{-in\phi}\ ds,$ (16)

the fractional change in $\beta(s)$ is given by

$$\frac{\Delta\beta}{\beta} = -\frac{\nu}{4\pi}\sum_{n=-\infty}^{\infty} \frac{J_n\ e^{in\phi}}{\nu^2 - (n/2)^2} \quad . \tag{17}$$

Using the modified beta function in eq. (8)

$$a_n \simeq -\frac{3\nu}{2\pi}\ \frac{J_n}{4\nu^2-n^2}\left(\frac{R}{\nu^3}\right)^{1/2} \quad . \tag{18}$$

2.3 Principle of changing the transition energy

The basic principle of changing the transition energy is to make a lattice of periodicity n and create a harmonic component a_n. A small value of a_n will bring a large change in γ_t from the unperturbed ($a_n = 0$) value $\gamma_t \simeq \nu$ if n is close to ν, (eq. (15)). This implies that the phase advance of each of n superperiods is close to 2π. To increase γ_t, n should be just above ν and to decrease it just below. If $\nu < n$ and the harmonic is strong enough then the momentum compaction factor may even become negative taking γ_t to an imaginary value.

The natural harmonic present due to the number of cells does not contribute significantly to γ_t since usually the tune of the machine is far away from this number.

It may be seen from eq. (8) that in order to generate an additional harmonic coefficient a_n, one has to modulate either β or $1/\rho$ or both. We shall go into more details of this in chapter 3.

2.4 Effects of changing transition energy on the lattice functions

In this section we shall examine the effects of various methods of changing transition energy on the lattice functions. A convenient measure to estimate the increase in the peak values of lattice functions is obtained when the magnitude of the harmonic is adjusted to bring α to zero. The value of $|a_n|$, from eq. (15), in that case will be

$$|a_n| = \frac{1}{\sqrt{2}}\left(\frac{R}{\nu^3}\right)^{1/2} \frac{|\nu^2-n^2|^{1/2}}{\nu} . \tag{19}$$

First we compute the change in the maximum value of beta function caused by the introduction of the harmonic modulations of periodicity n. This modulation, as a result, creates harmonics of order k = 0, n, 2n, 3n ... Therefore on expanding eq. (17), we obtain

$$\frac{\Delta\beta}{\beta} = -\frac{J_o}{4\pi\nu} + \frac{2\nu}{\pi}\frac{J_n}{4\nu^2-n^2}e^{in\phi} + \frac{2\nu}{\pi}\frac{J_{2n}}{4(\nu^2-n^2)}e^{2in\phi} + \frac{2\nu}{\pi}\frac{J_{3n}}{4\nu^2-9n^2}e^{3in\phi} + \ldots \tag{20}$$

Since ν is close to n it is important to make J_{2n} zero to avoid a large change in β. Therefore, assuming that J_{2n} is zero and that the magnitude of harmonics other than k = n is small, one obtains using eq. (18), (19) and (20)

$$\frac{\Delta\beta}{\beta} = \frac{2\sqrt{2}}{3\nu}(\nu^2 - n^2)^{1/2} \tag{21}$$

which shows that β will have a higher peak value unless ν is close to n.

The beta functions and tunes will change in only those schemes which involve the modulation of the focusing properties of the lattice. However, an unavoidable effect of changing γ_t, in any scheme, is the increase in the peak values (maximum and minimum) of the dispersion function η_x. In the presence of the harmonic components a_o and a_n (and therefore a_{-n}) only one obtains from eq. (2), (5), (9) and (12)

$$\eta_x = \left(\frac{\beta R}{\nu^3}\right)^{1/2} + \beta^{1/2}\frac{\nu^2}{\nu^2-n^2}\left(a_n e^{in\phi} + a_{-n}e^{-in\phi}\right). \tag{22}$$

while the original value of η_x when γ_t was not raised ($a_n = 0$) was given by

$$\eta_{xo} = \left(\frac{\beta_o R}{\nu^3}\right)^{1/2}, \tag{23}$$

with β_o the value of the beta function in that lattice.

Equations (21) to (23) give the fractional change in the peak values of the dispersion function.

$$\frac{\Delta\eta_x}{\eta_{xo}} = \pm\frac{\nu}{|\nu^2-n^2|^{1/2}}\left(\frac{2\beta}{\beta_o}\right)^{1/2} + \left[1 - \left(\frac{\beta}{\beta_o}\right)^{1/2}\right]$$

$$\simeq \pm\frac{\sqrt{2}\,\nu}{|\nu^2 - n^2|^{1/2}} \tag{24}$$

neglecting the change in β (eq. (21)). The equation again exhibits the need of staying away from ν = n to avoid the large peak values of the dispersion functions.

Thus we see that to avoid higher β, ν should be close to n (eq. (20)) and to avoid higher η_x (eq. (24)) ν should be away from n. Therefore a suitable value of ν/n should be chosen to make a proper compromise.

The change in tune ν can be computed by using eq. (4.35) to eq. (4.37) of Courant and Snyder[4].

3. Methods to design a high transition energy lattice

In this chapter we look at ways of creating the harmonic component responsible for producing high transition energy in a lattice. It is presumed that ν is close to but less than n unless otherwise mentioned. It may be recalled that for obtaining the harmonic coefficient a_n one has to modulate either β (the focusing properties) or $1/\rho$ (the bending properties) or both. We divide all methods in three basic approach and discuss a few possible variations in these approaches in the relevant sections.

3.1 Reverse field magnets

The first published proposal[8] for a high transition energy lattice was based on using a number of reverse field magnets. These magnets have the same field index but they bend in the opposite direction giving $1/\rho$ a negative value. This generates a harmonic coefficient due to the variation in $1/\rho$. The obvious disadvantage of this scheme lies with the considerable increase in circumference. In the Serphukov synchrotron for which this method was proposed, approximately an extra 25% magnet length was required.

3.2 Pairs of trim quadrupoles

In this method a pair of focusing (F) and defocusing (D) quadrupoles is used in each superperiod to modulate the beta function. The F and D quads are placed at about a phase of π apart and a small difference in β around the two quads generates the desired harmonic. A detailed analysis of the scheme has been made by Ohnuma[9], Teng[10,11] and also by Hardt[7] using a somewhat different approach. The method has also been used in the proposed lattice for SIS 12/18[12]. Ohnuma treats the trim quadrupoles as an error in field gradients and obtains

$$\frac{1}{\gamma_t^2} \simeq \frac{1}{\nu^2}\left[1 + \frac{9\nu^4}{2\pi^2}\sum_{k>o} \frac{|J_k|^2}{(\nu^2-k^2)(4\nu^2-k^2)^2}\right], \tag{28}$$

where J_k has been defined in eq. (16).

It appears from this equation that the component J_n with $n \simeq 2\nu$ will be more effective in bringing a large change in γ_t than J_n with $n \simeq \nu$. But eq. (17) indicates that if $n \simeq 2\nu$ the change in β will be very large and therefore in that case this equation and the above expression for γ_t will no longer be valid. We found that it was practically impossible to change γ_t by a very large amount using this component only.

The above component ($n \approx 2\nu$) in fact should be avoided in the lattice to keep the maximum beta low. We use an unequal excitation of the trim quads to eliminate this component. If the strength of the two trim quads (F and D) are $k + \delta k$ and $-k + \delta k$ then k contributes mainly for J_n and δk to J_{2n}. The magnitude of the inequality in the excitation of the two trim quads may be used as a fitting variable to keep β almost unchanged at the point exactly in between the two quads.

In a first lattice design[1] for the TRIUMF Kaon factory this method was used with $\nu \approx n$ for taking γ_t to ~ 35 with maximum beta (both β_x and β_y) ~ 40 m. However, this lattice had an inherent $n \approx 2\nu$ harmonic. By an unequal excitation of trim quads both β_x and β_y were made < 32 m while raising γ_t to an imaginary value. The maximum β in the same lattice with no excitation of trim quads was about 30 m.

Probably the most straightforward way to modulate β functions in a lattice is to modulate the strength of main quadrupoles themselves. This changes γ_t without increasing the total length of quadrupoles in the machine (a relatively small increase in strength may be required to compensate the small change in ν). A lattice based on this scheme is given in fig. 2. The length of all four horizontally focusing quads in a lattice with $\gamma_t \approx \nu$ was 1.7 m. To increase γ_t to an imaginary value the length of two of these quads (which are approximately π phase apart) may be changed to 1.4 m and 2.0 m respectively. However, in the lattice of fig. 2 the lengths are changed to 1.45 m and 1.98 m respectively to suppress J_{2n}, as mentioned earlier. The maximum magnetic field in the magnet is 1.65 T and in the quad 1.2 T. The length of all magnets is 2 m and of drifts 0.5 m.

3.3 Modulation of the magnet distribution

In this section we discuss the methods of modulating $1/\rho$ without using the reverse field magnets. In part (a) the missing magnet cells method is discussed for modulating $1/\rho$ without affecting the beta functions. This method has been used for the SATURNE II[13] lattice and for a 3 GeV booster at TRIUMF. In part (b) we combine the modulation in β to $1/\rho$ to increase the magnitude of the harmonic coefficient $|a_n|$.

3.3(a) Missing magnet cells

The harmonic component a_n due to $1/\rho$ variation can be generated by making a lattice in such a way that a relatively long section with no magnets is created around one place in each of n superperiods.

We consider an example in which a superperiod is made of p cells of which e are empty (no magnets, $1/\rho = 0$). We obtain approximate expressions for γ_t and other quantities. Making an approximation in eq. (8) by replacing β by its average value R/ν we obtain

$$a_n \approx \frac{1}{2\pi}\left(\frac{R}{\nu}\right)^{3/2} \int_{-\pi}^{\pi} \frac{1}{\rho}\, e^{-in\phi}\, d\phi = \frac{n}{2\pi}\left(\frac{R}{\nu}\right)^{3/2} \int_{-\pi/n}^{\pi/n} \frac{1}{\rho}\, e^{-in\phi} d\phi,$$

since we have n superperiods. If the superperiod has a reflection symmetry about the origin

$$a_n \simeq \frac{n}{\pi}\left(\frac{R}{\nu}\right)^{3/2} \int_0^{\pi/n} \frac{1}{\rho}\cos n\phi \, d\phi = \frac{1}{\pi}\left(\frac{R}{\nu}\right)^{3/2} \int_0^{\pi} \frac{1}{\rho}\cos \zeta d\zeta ,$$

where the new variable $\zeta = n\phi$ ranges from $-\pi$ to π in a superperiod. $1/\rho$ is zero in the empty cells and we can put approximately $R/\rho = p/(p-e)$ in the cells with magnets and obtain

$$a_n \simeq - \frac{\sin(\pi\ e/p)}{\pi} \ \frac{R}{\nu^3}^{1/2} \ \frac{p}{p-e} \ . \tag{29}$$

The actual circumference factor should be used for R/ρ if the lattice is not tightly packed.

Replacing a_n by this value in (15)

$$\frac{1}{\gamma_t^2} \simeq \frac{1}{\nu^2}\left[1 + 2\,\frac{\sin^2(\pi\ e/p)}{\pi^2}\left(\frac{p}{p-e}\right)^2 \frac{\nu^2}{\nu^2-n^2}\right], \tag{30}$$

and similarly in (19)

$$\eta_x(\phi) = \left(\frac{\beta R}{\nu^3}\right)^{1/2}\left[1 - 2\,\frac{\sin(\pi\ e/p)}{\pi}\left(\frac{p}{p-e}\right)\frac{\nu^2}{\nu^2-n^2}\cos n\phi\right] \tag{31}$$

These approximate expressions predict results quite close to the values given by the computer code DIMAT[15], particularly when the cells with the magnets are tightly filled. A lattice based on this scheme is given in fig. 3 where one of the four cells is empty; the number of superperiods is 12 and ν_x is 10.9143. The maximum magnetic field used in the magnets is 1.75 T and in quads 1.2 T. The lengths of all magnets is 2.5 m and of quads 1.5 m. The drift space between the quad and magnet is 0.5 m and between two magnets 0.3 m. In fig. 4 values of γ_t and η_x predicted by eq. (30) and eq. (31) are compared with those given by DIMAT. The variable on the x-axis is ν_x/n which is varied by changing the strength of the quads in the lattice of fig. 3. The empty cell can center either around an F quad or a D quad. The maximum value of η_x in the lattice is lower if it is around a D quad. However, the maximum value of η_x in the magnets is lower if it is around an F quad.

3.3 (b) Unequal Drift Lattice

The modulation in $1/\rho$ can also be obtained by modulating the strength or the distribution of the bending fields. This, for example, may be achieved by shifting the magnets in such a way that they get crowded around one point and get further away from another point (which is about π phase away from the first).

In a combined function machine the shift of the magnets causes a modulation in β as well. These two modulations (β and $1/\rho$) can be used together to get a higher value of the fourier coefficient a_n. An example of this scheme is given in fig. 10 and is explained in detail in chapter 4.

The scheme of using the two modulations (β and $1/\rho$) can obviously be employed more efficiently in a separated function machine to obtain high γ_t with modest peak values of β_x, β_y and η_x. On the other hand this approach can also be utilized in making a compact dispersion suppressor for the lattices of high η_x. In one example we were able to bring $\eta_x = 5.7$ m to zero by using a half empty cell and the modulation in the quad strength.

4. Lattice design for the 30 GeV Synchrotron

In this section we describe a lattice for the proposed 30 GeV synchrotron. We explain how the desired harmonic for the high transition energy is created and how various parameters are optimized.

The regular lattice (all drifts equal, $\gamma_t \simeq \nu$) and the plot of its lattice functions are shown in fig. 1. This lattice is constructed of the so called long F and long D blocks with each long block consisting of two identical magnets HFL or HDL. In these long blocks the two magnets have a common coil and therefore the separation between the two is fixed. However, in the short blocks, HFS or HDS, each magnet has a separate coil and therefore the separation between the two HFS or HDS can be varied.

The regular lattice has 48 cells and each cell has a phase advance close to but below $\pi/2$. For a high γ_t lattice we take a superperiod of four basic FODO cells and shift the magnets to produce

```
1                   2
↓                   ↓
F O O D O F O O D O F O D O O F O D O O

   ___       ___          ___       ___
   ↓    ↓    ↓    ↓   ↓    ↓    ↓    ↓
   a    b    c    d   d    c    b    a
```

where a single O represents a short drift (S) and two O's, a long drift (L), and where 1 and 2 are the two reflection symmetry points. The magnets are shifted symmetrically away from 1 and towards 2, thus modulating both the bending and the focusing properties of the lattice.

It can be seen from eq. (8) that to obtain a high harmonic coefficient $|a_n|$, both $\beta^{3/2}$ and $1/\rho$ should be high around 2 and low around 1 (or vice versa). In the above structure decreasing the length of drifts d increases the magnet density around 2, making $1/\rho$ higher; conversely increasing drifts a makes magnet density and $1/\rho$ lower around 1. It may also be noticed that the short drifts d increase the defocusing (or decrease the focusing) around 2 (by bringing the D magnets closer to it) and thereby make $\beta^{3/2}$ higher; conversely the longer drifts a make $\beta^{3/2}$ lower around 1. Thus for designing a high transition energy lattice in this scheme, the drifts a should be longer and d shorter. Also the F magnets should be at the symmetry points; D magnets at the symmetry points will change $\beta^{3/2}$ and $1/\rho$ in opposite senses. One may find several possible combinations of the four drifts "a b c d" satisfying this requirement; some of the drift patterns for them are:

"LSLS" , "LLSS" , "LMMS" , etc.

Here S, M and L stand for short, medium and long drifts, M being taken equal to the drift length of the regular lattice. The variation of γ_t with (L-S) between these patterns is shown in fig. 5.

These changes in the lattice structure also cause changes in the tunes and in the lattice functions. In fig. 5 ν_x and $\hat{\eta}_x$ are also plotted (together with γ_t) against (L-S). The variation of ν_x with (L-S) is different in these patterns, it decreases in pattern LSLS but increases in LMMS and LLSS, more rapidly in LLSS. This difference is important due to the presence of the factor $1/(\nu^2-n^2)$ in the expressions for γ_t and $\hat{\eta}_x$ (eq. (15 and (22)) and especially where ν is close to n. The decrease in ν with increasing (L-S) in pattern LSLS becomes so large that despite an increasing $|a_n|$, $\hat{\eta}_x$ eventually decreases. However, γ_t continues to increase because the factor $1/(\nu^2-n^2)$ is multiplied by $|a_n^2|$ in the expression of γ_t (whereas it is multiplied by a_n in the expression for $\hat{\eta}_x$). In fig. 6 $\hat{\beta}_x$ and $\hat{\beta}_y$ are plotted against (L-S) for these patterns.

Figure 7 shows the effect of an increase in the drift b and a decrease in c starting with pattern LSLS. This changes the pattern to LMMS and eventually to LLSS. The behavior of γ_t, $\hat{\beta}_x$, $\hat{\beta}_y$, $\hat{\eta}_x$, ν_x and ν_y against (c-b) is plotted in this figure for the fixed value of (a-d) = 3 m. The variation of γ_t and $\hat{\eta}_x$ in terms of a_n and ν_x has been explained above. The increase in the peak value of β_x (β_y) is associated with the J_{nx} and ν_x (J_{ny} and ν_y) as given in eq. (17). The major contributing harmonics are those of n close to ν and 2ν (in our case 12th and 24th harmonics). In the table below we give very approximate values of J_{12} and J_{24} in horizontal and vertical planes. They are computed under the assumption that the gradients of all combined function magnets can be substituted for the gradient errors in the calculation of 12th and 24th harmonic in eq. (16). We have also used β of the modified lattice instead of that of a regular lattice. The values of a_{12} and a_{24} are also given in this table. They are computed using eq. (8).

Table 1

S.No.	(c-b) (m)	a_{12} ($m^{1/2}$)	J_{12x} (m)	J_{12y} (m)	a_{24} ($m^{1/2}$)	J_{24x} (m)	J_{24y} (m)
1	-3	-0.092	-95	185	0.008	20	-18
2	-2	-0.078	-60	166	0.01	33	-86
3	-1	-0.069	-18	157	0.033	102	-38
4	0	-0.067	47	183	0.069	257	130
5	1	-0.067	169	296	0.149	563	438
6	2	-0.062	549	709	0.338	1461	1210

For β to be low both J_{12} and J_{24} (more important J_{24}) should be small. We see in fig. 7 that β is low when both 12th and 24th harmonics are small.

The harmonic modulation in $1/\rho$ in structure LSLS can be further augmented by increasing the first long drift a and decreasing another long drift c. The effect of this variation on various parameters is shown in fig. 8.

For the main ring structure LSLS is preferred because (a) it gives 2 long drifts in every half superperiod (24 in full machine) (b) it has the lowest β_x and η_x. The present lattice is actually a slightly modified version of LSLS type. This modification was done to obtain high enough γ_t and also to further optimize the lattice functions. The layout of this lattice is shown in fig. 9 and the lattice functions are plotted in fig. 10. The parameter list is given in Table 2.

Table 2

Parameter list for the 30 GeV Main Ring

1. Machine Structure Parameters

List of machine components in one superperiod:

FDR1 HFL FD11 HDL FDR1 FDR1 HDL FD22 HFL FDR1
FDR1 HFL FD33 HDL FDR1 FDR1 HDL FD44 HFL FDR1
FDR1 HFL FD44 HDL FDR1 FDR1 HDL FD33 HFL FDR1
FDR1 HFL FD22 HDL FDR1 FDR1 HDL FD11 HFL FDR1

(where the elements whose name begins with F are the drift spaces and with H are the magnets. Values of length, etc. of these elements are given below).

Circumference	:	826.87 meter
# Superperiods	:	12
# Cells	:	48
# Magnets	:	192
Maximum magnetic field in the magnet	:	1.35 Tesla

Length, bend angle and the field index of the magnets:

Magnet	Effective length (m)	Bend angle (deg)	Field index
HFL	2.5109	1.88145	-229.3925
HDL	2.4856	1.86855	218.7433

Length of the drift spaces (m)

FD11 (=a)	:	5.6278
FD22 (=b)	:	2.3377
FD33 (=c)	:	4.6378
FD44 (=d)	:	1.5477
FDR1	:	0.0395

2. Beam Dynamics Parameters

Horizontal tune	:	10.98
Vertical tune	:	9.87
Max. β_x	:	30.5 m
Max. β_y	:	37.7 m
Max. η_x	:	7.6 m
Min. η_x	:	-4.2 m

3. Extraction System Parameter

# Kicker magnets	:	2
# Septum magnet	:	1

Length, Deflection and the magnetic field in the kicker and the septum magnet

	Length	Deflection	Magnetic field
Kicker	4.5 m	1.35 m rad	.03 T
Septum	3.5 m	17.5 m rad	.5 T

Conclusions

Several methods of raising the transition energy of a lattice have been explored and the effects on the lattice functions examined. For the main ring of the TRIUMF Kaon Factory with combined function CERN/ISR magnets a lattice with modulated drift spaces seems to be the most attractive one. It eliminates the need for extra straight sections and does not require additional trim quadrupoles.

In a separated function machine, particularly for higher energy, a modulation in quadrupole strength seems to be the most straightforward and appealing method. In a lower energy machine, the 3 GeV Booster for example, the missing magnet method coupled with a modulation in quadrupole strength may be more suitable.

To keep the maximum value of the dispersion function low the number of superperiods should not be too close to the horizontal tune of the machine even if it requires a higher modulation. Though a proper choice will depend on a particular lattice we find that an optimum value of the tune per superperiod lies usually between .85-.95.

The harmonic component with ν close to $n/2$ must be suppressed to avoid an unnecessary increase in the maximum value of beta functions in the schemes involving a modulation in the focusing properties.

References

1. Progress Report on feasibility of using the ISR magnets in a TRIUMF Kaon Factory, June 1983.

2. H.G. Hereward, private communication, 1983.

3. R.C. Gupta, "Straight Section Designs", TRI-DN-83-31.

4. E.D. Courant and H.S. Snyder, "Theory of Alternating Gradient Synchrotron", Annals of Physics, vol. 3 (1958) 42.

5. V. Veksler, Journal of Physics 9 (1945) 153.

6. E.M. McMillan, Physical Review 70 (1945) 69.

7. W. Hardt, "Gamma Transition jump scheme of the CPS", Proceedings of IX International Conference, SLAC (1974) 434.

8. V.V. Vladimirski and E.K. Tarasov, "Problems of Cyclic Particle Accelerators", USSR Academy of Sciences, Moscow, 1955.

9. S. Ohnuma, Fermilab $\bar{p}$ note No. 105, Dec. 1980. (Also LA. - 9511 - C; Proceedings of the workshop on LAMPF II synchrotron, Jan. 1983).

10. L.C. Teng, NAL, FN-207, April 1970.

11. L.C. Teng, NAL, TM-276, Nov. 1970.

12. B. Franczak, K. Blasche, K.H. Reich, Particle Accelerator Conference (1983) 2120.

13. J.L. Laclare, SATURE, in MARIA design symposium, Vol. III, Edmonton (1980) 55.

14. R.C. Gupta "Methods of Designing Synchrotrons with High Transition Energy", TRI-DN-83-36.

15. R. Servranckx, " Lattice code DIMAT". Userguide will be available as a SLAC PEP note in summer 1984.

Appendix A

Extraction System for the unequal drift lattice

Here we briefly describe a fast extraction system which fits into the long drifts of the unequal drift lattice to take the beam out of the machine in a single turn.

The extraction system is designed for a beam of emittance 12.5 π mm mrad and consists of two kicker magnets and one septum magnet. The maximum magnetic fields to be used in the kicker and in the septum magnets are respectively .03T and .5T. Both kickers are 4.5 m long and give the beam an outward deflection of 1.35 m rad. The second kicker is located about 2π phase advance apart from the first kicker and the combined deflection takes the whole beam to the other side of the septum magnet, which always stays out of the path of the circulating beam. When this beam arrives at the 3.5 m long septum, it already has a clear separation of 1 cm from the original circulating beam and gets an additional deflection of 17.5 m rad to get completely out of the synchrotron.

The extraction system is shown in fig. 11 where the envelopes for the deflected and the normal circulating beams have been plotted.

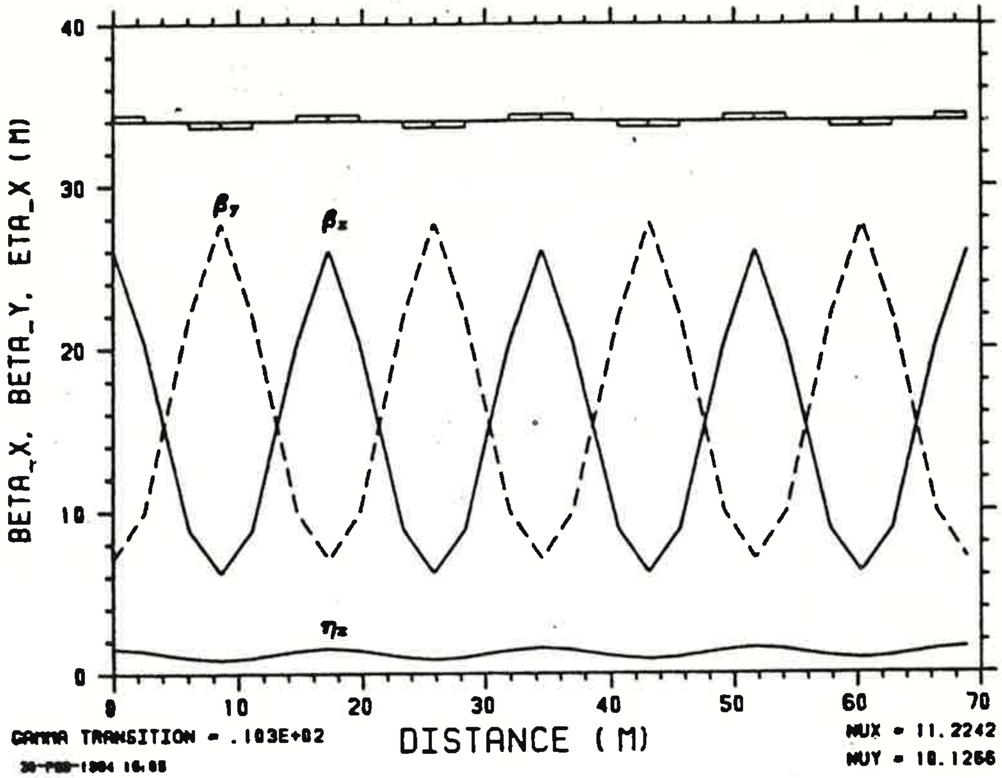

Fig. 1. Regular lattice consisting of CERN/ISR magnets. The transition energy is in the range of acceleration. (Ref. Ch. 1).

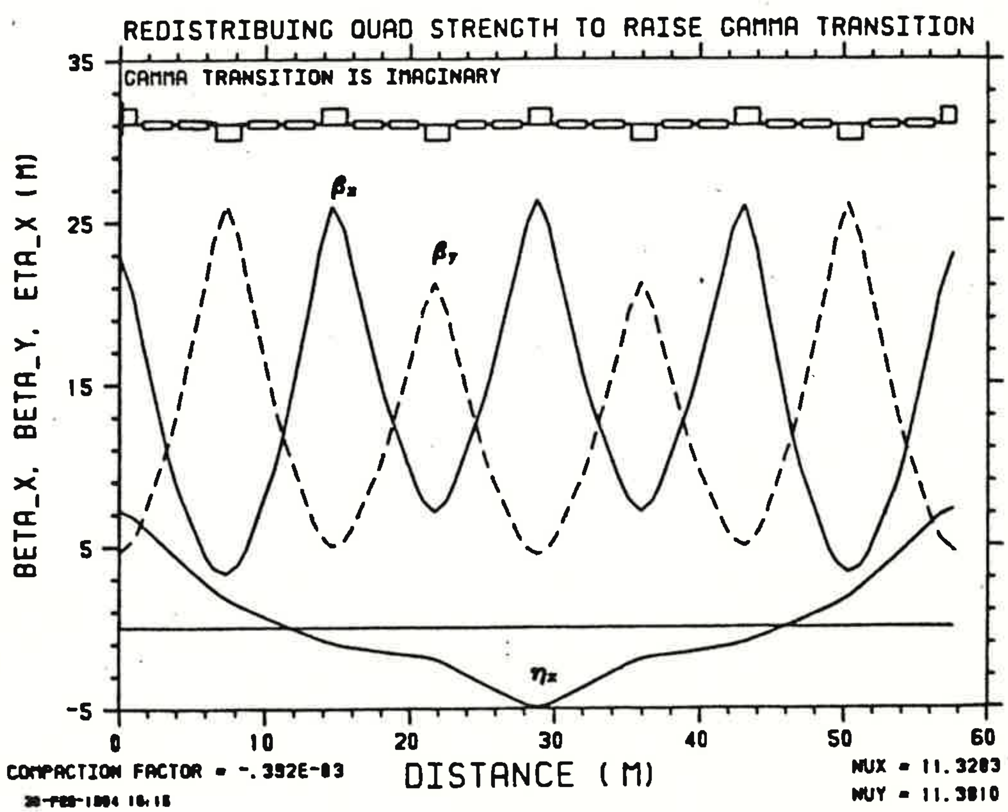

Fig. 2. Raising transition energy by modulating the quadrupole lengths. The length of the quadrupoles at the two symmetry points are respectively 1.98 m and 1.45. The compaction factor has become negative and γ_t imaginary. Length of all quads in a regular lattice will be 1.7 m. (Ref. Sec. 3.2).

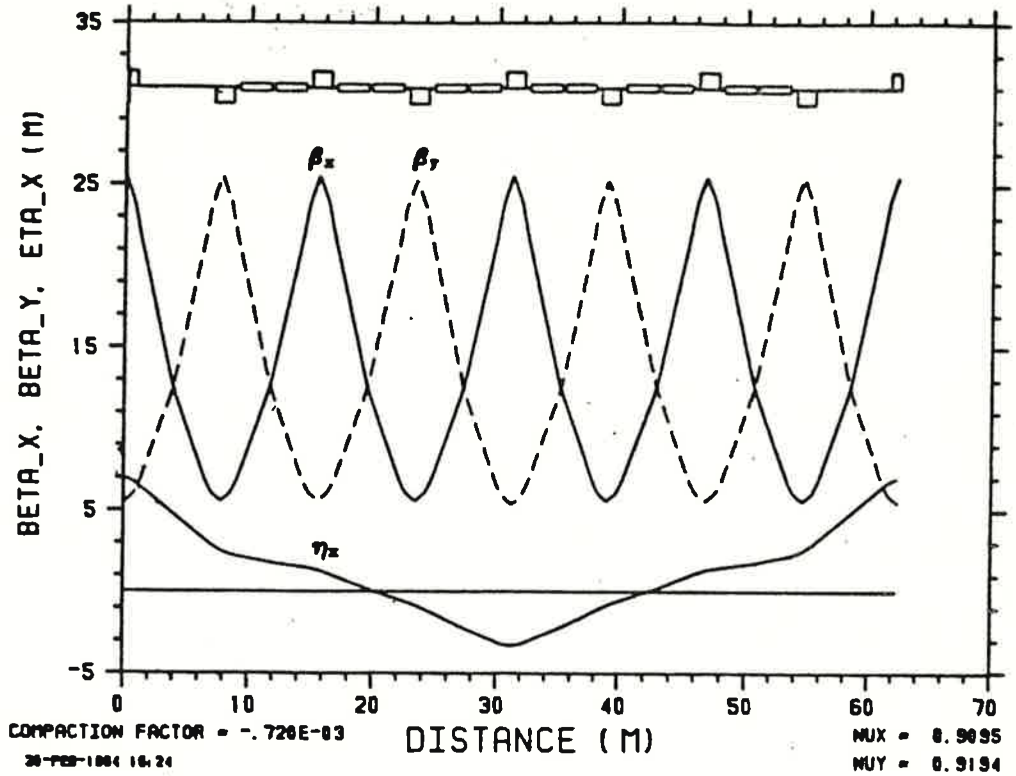

Fig. 3. Raising transition energy using missing magnet cells. In this example one of the four cells is empty. ν_x/n is .9095 and n, the no. of superperiods, is 12. (Ref. Sec. 3.3 (a)).

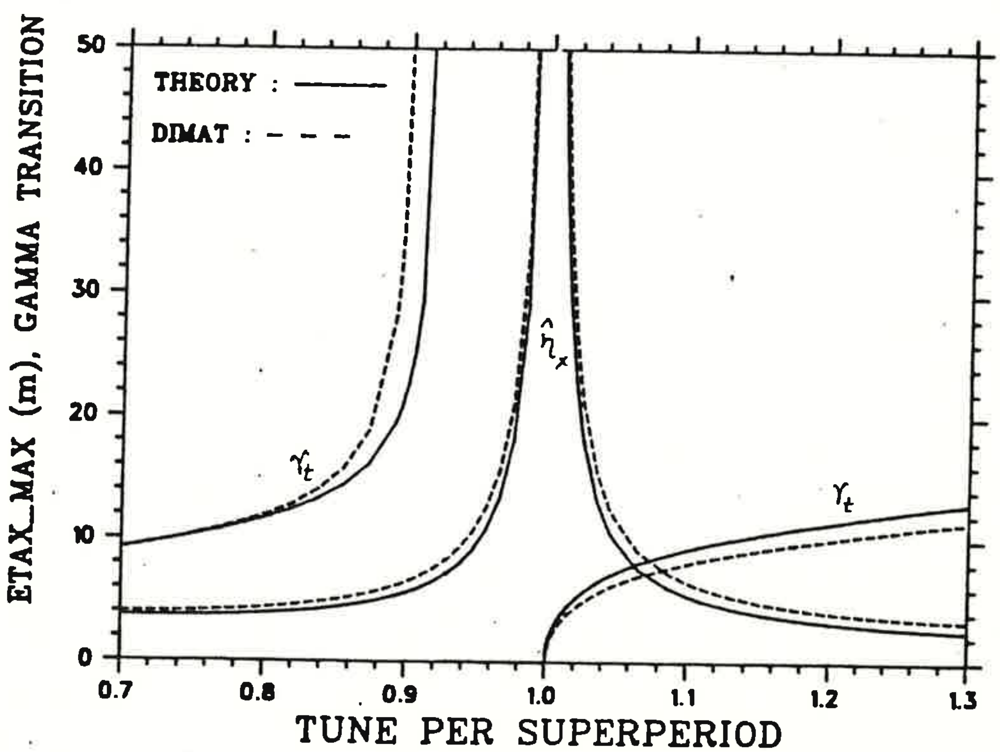

Fig. 4. Comparison of the dispersion and γ_t for the computed results using the formulas derived in Sec. 3.3 (a) and the results obtained from the lattice code DIMAT in the missing magnet cells method. (Ref. Sec. 3.3 (a)).

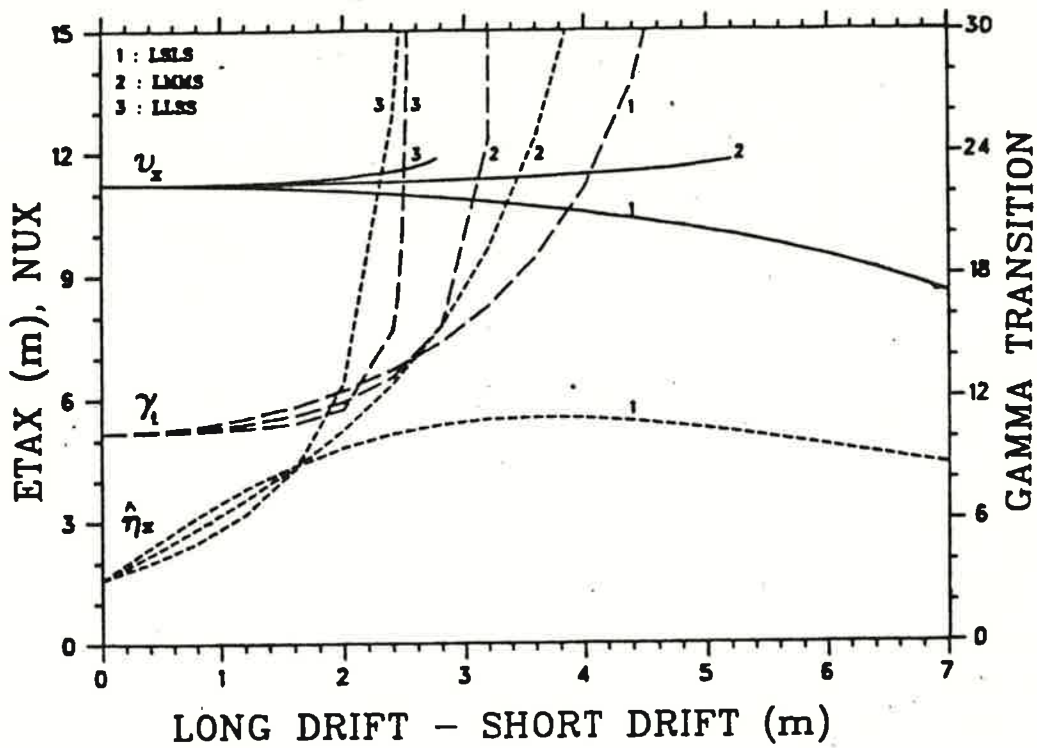

Fig. 5. Effects of increasing the difference between the long and the short drifts starting from a regular lattice. Patterns examined: 1:LSLS, 2:LMMS and 3:LLSS (M = 3.5 m = drift length in a regular lattice). In this figure ν_x, $\hat{\eta}_x$ and γ_t are shown (Ref. Ch. 4).

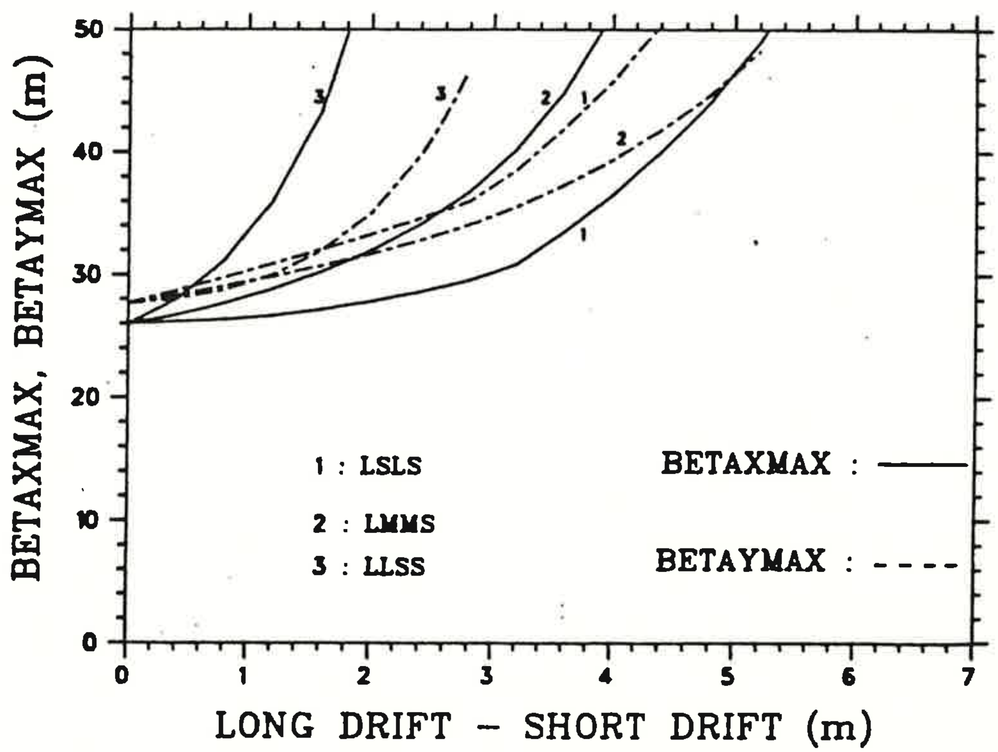

Fig. 6. Same as Fig. 5 but behaviour of $\hat{\beta}_x$ and $\hat{\beta}_y$ is shown. (Ref. Ch. 4).

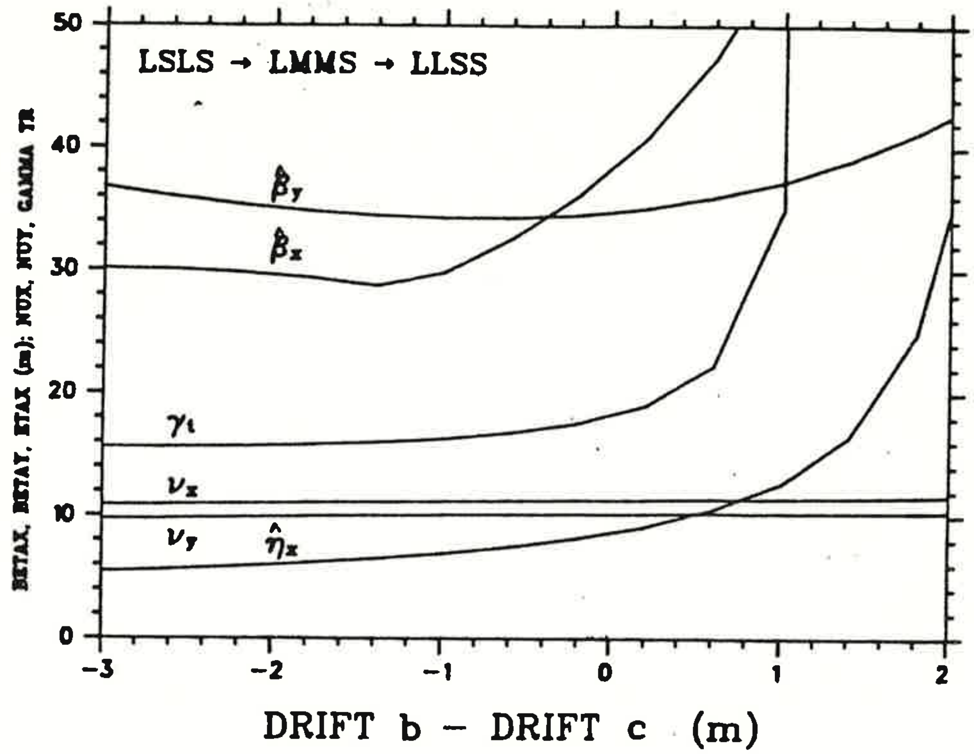

Fig. 7. Behaviour of lattice functions:
Starting from the pattern LSLS (for drifts abcd), the difference between the drifts b and c is increased. It changes the pattern LSLS to LMMS (when b-c = 0 m) and eventually to LLSS (when b-c = 3m; however, the motion becomes unstable before that). (Ref. Ch. 4 and see also Table 1).

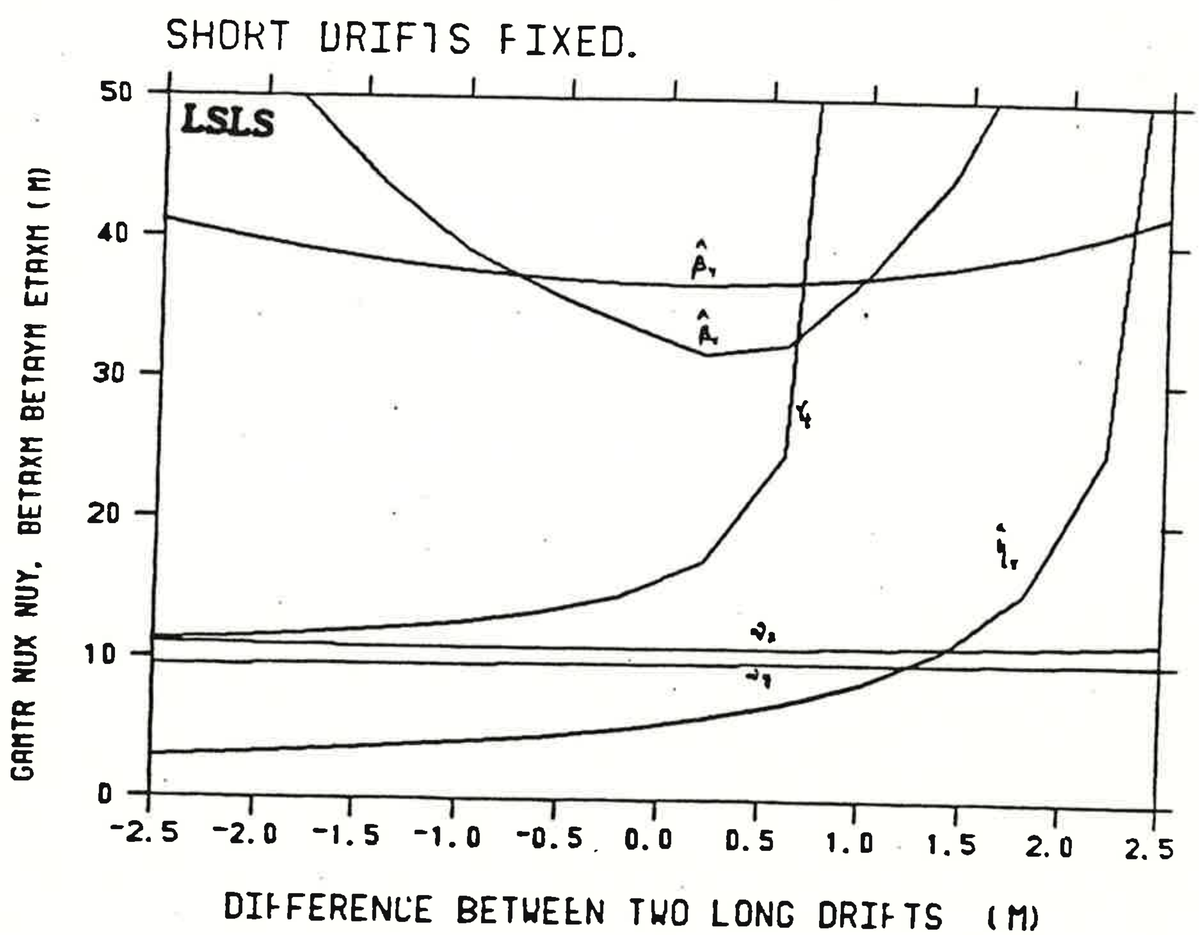

Fig. 8. The difference between the two long drifts a and c (in the pattern LSLS) is increased to enhance the modulation in $1/\rho$ to further increase γ_t. Ref. (Ch. 4)).

ONE SUPERPERIOD OF THE 30 GEV MAIN SYNCHROTRON

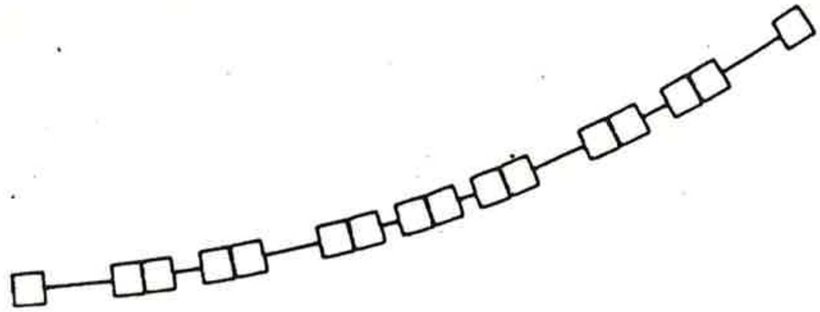

Fig. 9. Layout of one superperiod. A relatively higher magnet density is created at the mid-point. This provides the desired harmonic to increase γ_t, (see lattice below). There are 12 superperiods in the main synchrotron. (Ref. Ch. 4).

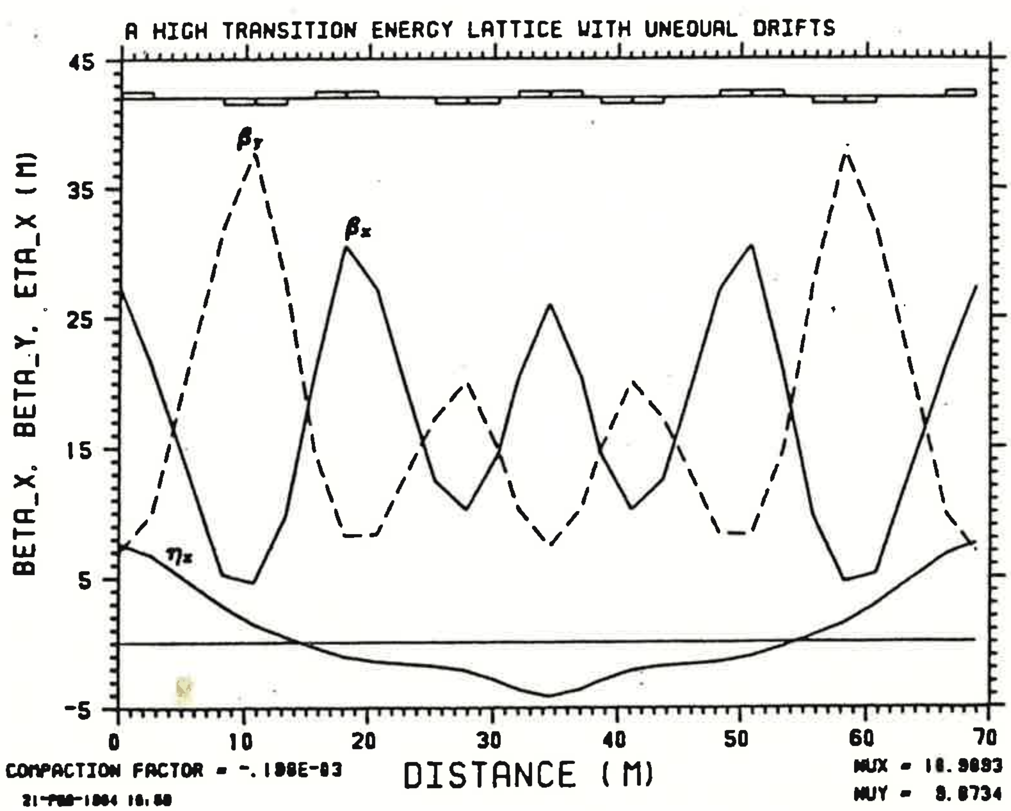

Fig. 10. A lattice optimized for high transition energy and low peak values of the lattice functions. A complete parameter list is given in Table 2. (Ref. Ch. 4).

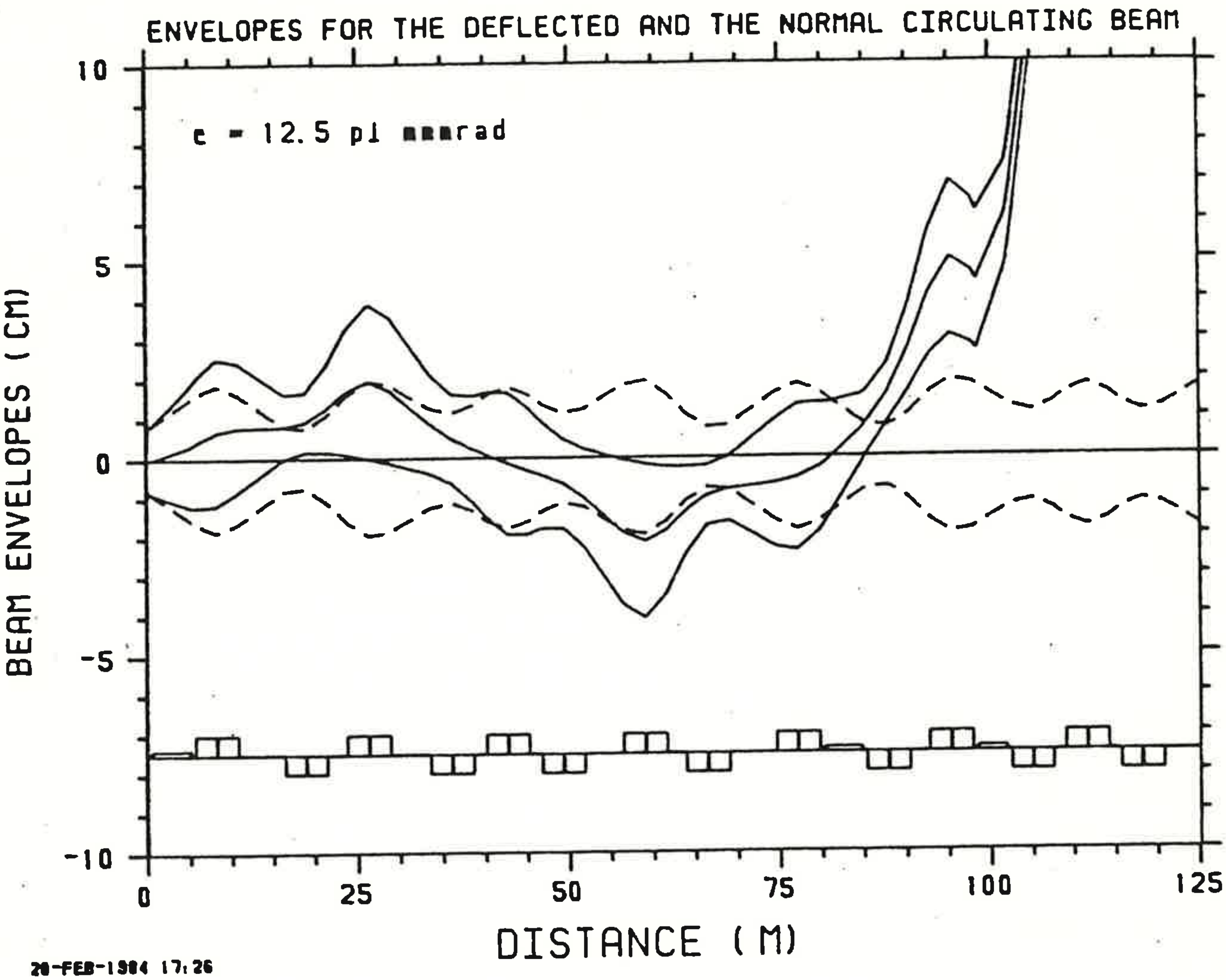

Fig. 11. A fast extraction system for the main synchrotron. Long drifts of the unequal drift lattice of Fig. 10 have been utilized for placing the two kickers and one septum magnet. (Ref. Appendix A).